DIAGNOSTIC NEURORADIOLOGY

CrossMark

Dynamic susceptibility contrast and diffusion MR imaging identify oligodendroglioma as defined by the 2016 WHO classification for brain tumors: histogram analysis approach

Anna Latysheva[1] · Kyrre Eeg Emblem[2] · Petter Brandal[3] · Einar Osland Vik-Mo[4,5] · Jens Pahnke[6,7] · Kjetil Røysland[8] · John K. Hald[1] · Andrés Server[1]

Abstract

Purpose According to the revised World Health Organization (WHO) Classification of Tumors of the Central Nervous System (CNS) of 2016, oligodendrogliomas are now defined primarily by a specific molecular signature (presence of IDH mutation and 1p19q codeletion). The purpose of our study was to assess the value of dynamic susceptibility contrast MR imaging (DSC-MRI) and diffusion-weighted imaging (DWI) to characterize oligodendrogliomas and to distinguish them from astrocytomas.

Methods Seventy-one adult patients with untreated WHO grade II and grade III diffuse infiltrating gliomas and known 1p/19q codeletion status were retrospectively identified and analyzed using relative cerebral blood volume (rCBV) and apparent diffusion coefficient (ADC) maps based on whole-tumor volume histograms. The Mann-Whitney U test and logistic regression were used to assess the ability of rCBV and ADC to differentiate between oligodendrogliomas and astrocytomas both independently, but also related to the WHO grade. Prediction performance was evaluated in leave-one-out cross-validation (LOOCV).

Results Oligodendrogliomas showed significantly higher microvascularity (higher $rCBV_{Mean} \geq 0.80$, $p = 0.013$) and higher vascular heterogeneity (lower $rCBV_{Peak} \leq 0.044$, $p = 0.015$) than astrocytomas. Diffuse gliomas with higher cellular density (lower $ADC_{Mean} \leq 1094 \times 10^{-6}$ mm^2/s, $p = 0.009$) were more likely to be oligodendrogliomas than astrocytomas. Histogram analysis of rCBV and ADC was able to differentiate between diffuse astrocytomas (WHO grade II) and anaplastic astrocytomas (WHO grade III).

Conclusion Histogram-derived rCBV and ADC parameter may be used as biomarkers for identification of oligodendrogliomas and may help characterize diffuse gliomas based upon their genetic characteristics.

Keywords Diffuse glioma · Perfusion MRI · Diffusion MRI

✉ Anna Latysheva
alatysheva@ous-hf.no

1. Department of Radiology, Oslo University Hospital—Rikshospitalet, 4950 Nydalen, 0424 Oslo, Norway

2. Department of Diagnostic Physics, Oslo University Hospital—Rikshospitalet, Oslo, Norway

3. Department of Oncology, Oslo University Hospital—Radiumhospitalet, Oslo, Norway

4. Department of Neurosurgery, Oslo University Hospital—Rikshospitalet, Oslo, Norway

5. Faculty of Medicine, University of Oslo, Oslo, Norway

6. Department of Neuro-/Pathology, Translational Neurodegeneration Research and Neuropathology Lab, University of Oslo and Oslo University Hospital, Oslo, Norway

7. University of Lübeck, LIED, Lübeck, Germany

8. Department of Biostatistics, Institute of Basic Medical Sciences, University of Oslo, Oslo, Norway

Introduction

Increasing evidence suggests that the presence of certain genetic aberrations in diffuse gliomas significantly improves prognostic accuracy compared to a diagnosis based exclusively on histology. Several large clinical trials have demonstrated more benefit from chemotherapy and better overall survival in patients with the presence of an IDH mutation and 1p19q codeleted gliomas (oligodendrogliomas) as compared to their genetic counterparts (astrocytomas). Differentiation between these two entities affects treatment strategy [1–4].

The revised fourth edition of the 2016 World Health Organization (WHO) Classification of Tumors of the Central Nervous System (CNS) incorporates genetic markers as the basis for classification [5]. For tumors harboring astrocytic and oligodendroglial elements, the genetic constitution will define it as an astrocytoma or oligodendroglioma [6, 7]. Specifically, diffuse gliomas with mutations in isocitrate dehydrogenase 1 or 2 (*IDH1* and *IDH2*) and whole-arm losses of 1p and 19q (1p/19q codeletion) will be classified as oligodendrogliomas, while those without 1p/19q codeletion will be classified as astrocytomas with or without *IDH1/2* mutation [5].

The current diagnostic standard for grading of diffuse glioma is histopathological evaluation of tissue specimens and molecular testing for the identification of genetic alteration (IDH1/2, IDH wild type, and 1p19q codeletion status). In cases with possible non-representative biopsy sampling and/or conflicting molecular results, it is important to identify robust non-invasive biomarkers that may help guide clinical decision making [6, 8].

Dynamic susceptibility contrast MR imaging (DSC-MRI) and diffusion-weighted imaging (DWI) are widely used techniques in brain tumor diagnostics. They allow characterization of specific tumor components, as well as functional signatures of the entire tumor and surrounding tissue. Relative cerebral blood volume (rCBV) from perfusion MRI is a reliable biomarker used to assess tissue vascularity and, what is most important for glioma grading, to estimate the apparent grade of neoangiogenesis [9–11]. Apparent diffusion coefficient (ADC) from DWI is used as a quantitative parameter to assess the grade of restrictive diffusion and to provide information about tissue structure and cellularity [12, 13].

Previous studies have demonstrated the ability of DSC and DWI to differentiate oligodendroglioma from astrocytoma, diffuse glioma WHO grade II from grade III, and 1p19q codeleted tumors from 1p19q non-codeleted tumors [14–19]. But in most studies which were performed prior to the updated WHO CNS tumor classification [20], oligoastrocytomas were included in oligodendroglioma's subgroup and were analyzed together. For this reason, non-invasive in vivo functional tissue information to compliment the new genetic entities

oligodendroglioma (IDH mutant, 1p19q codeleted) and astrocytoma (IDH mutant, non-1p19q codeleted) is necessary.

The purposes of this retrospective study were to determine whether the rCBV and ADC values analyzed by histogram methods could help to classify oligodendrogliomas from astrocytic tumors and to distinguish diffuse gliomas WHO grade II from grade III.

Material and methods
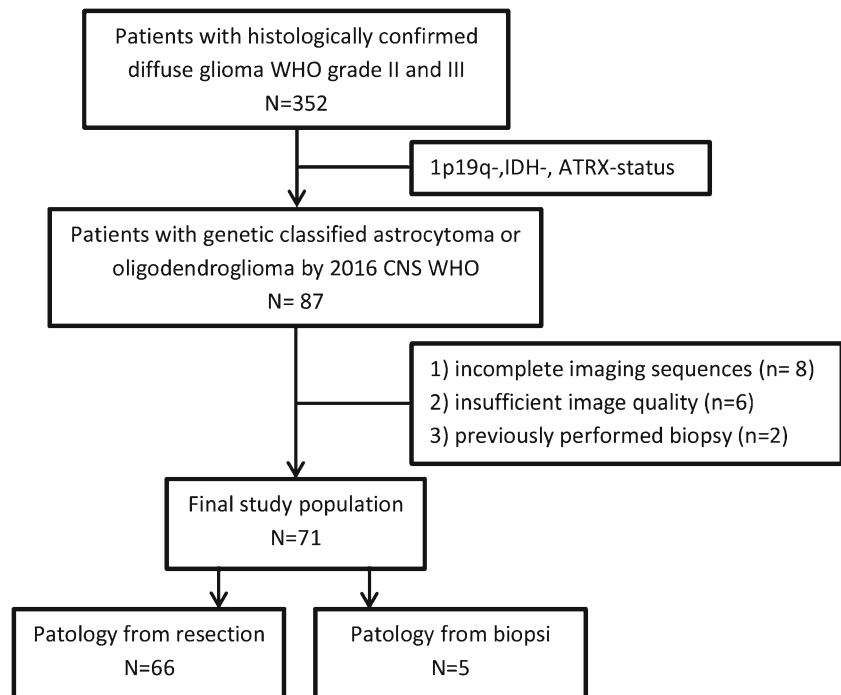
Patient selection

From November 2006 until May 2013, a total of 352 consecutive adult patients with a histopathologic diagnosis of diffuse glioma were identified based on our clinical database. Of these, 87 diffuse glioma grades II and III were diagnosed histopathologically as oligodendroglioma, oligoastrocytoma, or astrocytoma, classified according to the 2007 WHO Classification of Tumors of the CNS, were selected. Molecular genetic status with respect to 1p19q codeletion was available for all patients and met the following inclusion criteria: (1) a baseline pretreatment MRI examination from our institution including DSC-MRI and DWI in addition to T1-weighted and T2-weighted images, (2) age > 18 years, and (3) a signed consent. From this group, 71 were included in the final study cohort. The following patients were excluded: (1) incomplete imaging sequences ($n = 8$), (2) insufficient image quality ($n = 6$), and (3) previously performed biopsy ($n = 2$). The patient inclusion and exclusion process is shown in Fig. 1.

Histopathologic, molecular genetic analysis and classification

Tumor tissue obtained from needle biopsy or surgical excision, routinely formalin-fixed and paraffin-embedded (FFPE), was reviewed and diagnosed by experienced neuropathologists. All tumors were initially classified as oligodendroglioma, astrocytoma, or oligoastrocytoma according to WHO 2007. They were, thereafter, divided into genetically defined subtypes according to WHO 2016 criteria: (1) oligodendroglioma-grade II with 1p/19q codeletion, (2) anaplastic oligodendroglioma-grade III with 1p/19q codeletion, (3) diffuse astrocytoma-grade II without 1p/19q codeletion, and (4) anaplastic astrocytoma-grade III without 1p19q codeletion. Astrocytoma subtypes were also stratified as IDH1/2 mutant or IDH1/2 wild type when IDH1/2 status was known.

In the period from 2006 to 2009, routine 1p19q codeletion status analysis was performed by polymerase chain reaction (PCR) using at least four of six microsatellite markers on 1p35–36 and 19q13 [21]. From 2009 on, multiplex ligation-dependent probe amplification (MLPA) was performed for

Fig. 1 Patient flow diagram

```
┌─────────────────────────────────────┐
│ Patients with histologically confirmed │
│   diffuse glioma WHO grade II and III  │
│              N=352                    │
└─────────────────────────────────────┘
                │
                │────────┤ 1p19q-,IDH-, ATRX-status
                ▼
┌─────────────────────────────────────┐
│ Patients with genetic classified astrocytoma or │
│  oligodendroglioma by 2016 CNS WHO    │
│              N= 87                    │
└─────────────────────────────────────┘
                │
                │────────┤ 1) incomplete imaging sequences (n= 8)
                │        │ 2) insufficient image quality (n=6)
                │        │ 3) previously performed biopsy (n=2)
                ▼
       ┌──────────────────┐
       │ Final study population │
       │       N=71            │
       └──────────────────┘
          │            │
          ▼            ▼
┌──────────────┐  ┌──────────────┐
│ Patology from │  │ Patology from │
│ resection     │  │ biopsi        │
│ N=66          │  │ N=5           │
└──────────────┘  └──────────────┘
```

detection of 1p19q codeletion (SALSA MLPA probemix P088-C2), ATRX (SALSA MLPA P013 ATRX), TP53 (SALSA MLPA P056 TP53), IDH1 (isocitrate dehydrogenase 1 gene NM_005896.3), or IDH2 (isocitrate dehydrogenase 2 gene NM_005896.3) (SALSA MLPA P370 BRAF-IDH1-IDH2). MLPA is based on the ligation of two DNA oligonucleotides that hybridize adjacently to DNA target sequence and has previously been described [22]. The MLPA kit was assembled by MRC-Holland (Amsterdam, The Netherlands).

MR imaging

MRI was performed with a 1.5-T scanner (Sonata, Symphony, or Avanto; Siemens, Erlangen, Germany) equipped with an 8-channel (Sonata and Symphony imagers) or 12-channel (Avanto imager) phased-array head coil. The pretherapeutic MRI protocol included the following sequences: axial T2-weighted fast spin-echo (repetition time, TR 4000 ms; echo time, TE 104 ms; slice thickness, 5 mm; flip angel 146°), coronal fluid-attenuated inversion recovery (TR, 9000; TE, 108 ms; slice thickness, 5 mm; flip angel 120°), and axial T1-weighted spin-echo (TR, 500 ms; TE 77 ms; section thickness, 5 mm; flip angel 120°).

DWI was obtained using an axial echo-planar spin-echo sequence (TR, 2900 ms; TE 84 ms; section thickness 5 mm) before the injection of contrast agent. Diffusion was measured in three orthogonal directions using b values 0, 500, and 1000 s/mm^2.

Echo-planar gradient-echo DSC-MRI was acquired during contrast agent administration with TR, 1430 ms; TE 46 ms (12 axial sections) to TR, 1590 ms; TE 52 ms (14 axial sections);

bandwidth, 1345 Hz/pixel; voxel size, $1.80 \times 1.80 \times 5$ mm^3; intersection gap, 1.5 mm; 50 time points; flip angel 90°. After approximately eight time points, 0.2 mmol/kg of gadobutrol (Gadovist; Bayer Pharma AG, Berlin, Germany) was injected at a rate of 5 mL/s, immediately followed by a 20-mL bolus of NaCl (9 mg/mL) injected at a rate of at 5 mL/s. Post-contrast T1-weighted images were acquired after completion of the DSC-MRI [15].

Image processing

Data analysis was performed independently by two neuroradiologists and blinded to the histopathological and genetic/molecular characteristics. Tumor outlining and processing of ADC and rCBV maps were performed using nordicICE (NordicNeuroLab AS, Bergen, Norway). A series of ROIs were manually drawn on every representative slice for the entire tumor volume separately on ADC maps and T2-weighted images (Fig. 2). The borders were drawn at the transition between abnormal hyperintensity and normal parenchymal signal intensity based on visual evaluation with preferably avoidance of cystic components. The entire tumor volume includes both enhanced and non-enhanced components [23, 24]. Discrepancies were resolved by consensus reading.

Standard tracer kinetic models were used for creating CBV maps from DSC-MRI, corrected for potential contrast agent leakage from blood-brain barrier breakdown and normalized with respect to blood volume values from normal-appearing tissue to obtain relative CBV [24]. ADC maps from DWI were created using standard Stejskal-Tanner diffusion approximation [17, 25]. Whole-tumor normalized histogram
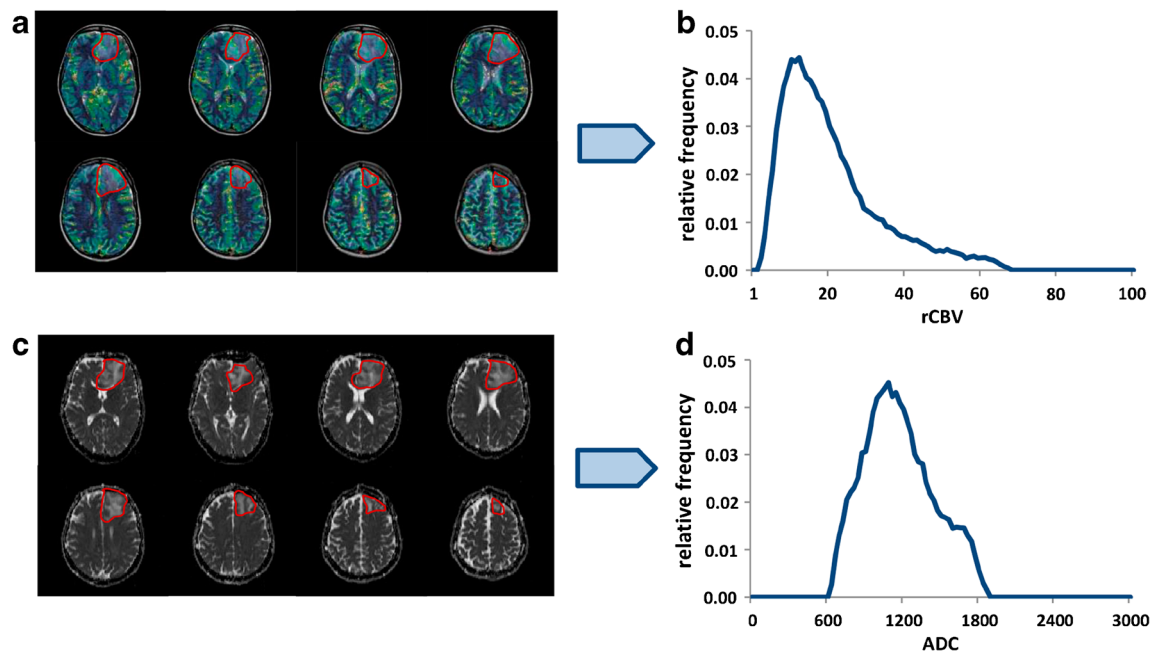
Fig. 2 Generation of rCBV and ADC histograms. Regions with signal hyperintensities were segmented on axial T2 images, coregistrated with rCBV maps and corresponding rCBV histogram in a 44-year-old woman with anaplastic oligodendroglioma (**a**, **b**). Total tumor volume was segmented on ADC maps in the same patient with corresponding ADC histogram (**c**, **d**)

distributions of the ADC and rCBV maps were created as described elsewhere [24]. In short, using MATLAB 2013 (MathWorks, Natick, Mass), 100 bin histograms were created over an ADC range of 0–300 and an rCBV range of 0–7.5 (ratios; arbitrary units), respectively. The histograms were normalized by making all areas under the curves equal to one to correct for varying tumor sizes [23]. To reduce the effect of outliers, all ADC and rCBV values below the 5% percentile and over the 95% percentile were excluded. The maximum peak heights of the normalized histogram (ADC_{Peak} and $rCBV_{Peak}$), as well as means of the tumor regions of interests (ADC_{Mean}, $rCBV_{Mean}$), were calculated. $rCBV_{Peak}$ and ADC_{Peak} were statistically used as measures of vascular and cellular tumor heterogeneity, respectively [17, 23].

Statistical analysis

The Mann-Whitney U test was used to assess ability of histogram-derived parameters to identify patients suggestive of an oligodendroglioma independent of histopathologic grade, but also in subgroups related to the WHO grade (II and III). The overall diagnostic performance was analyzed by the receiver operating characteristic curve (ROC), including values of sensitivity, specificity, and area under the curve (AUC). Optimal cutoff points based on the Youden index were also estimated. Association between genetically defined subtypes, WHO grade, and ADC and rCBV parameters was evaluated by both univariate and multivariate logistic regressions The leave-one-out cross-validation (LOOCV) algorithm was

used to estimate how accurately a predictive model differentiates between glioma subtypes. For all cases, an analysis value of less than 0.05 was considered to indicate a significant difference. The Holm-Bonferroni correction was used to control for multiple comparisons. Statistical analysis was performed using SPSS version 18 software (SPSS, Chicago, USA) and R version 3.3.3 (R Project for Statistical Computing; http://www.r-project.org).

Ethical consideration

Institutional and regional medical ethics committees approved this study (REC-number 2013/81 2.2006.541).

Results

Study population

Seventy-one patients (37 women, 34 men; median age, 48 years; range, 18–82 years) with diffuse infiltrating glioma grade II and III met all inclusion criteria and made up the study population. 1p19q status was considered for all patients, and IDH profile (IDH1 mutated, IDH2 mutated, or IDH wild type) was determined for 57.7% of the cases. We found that 28% of previously diagnosed oligodendrogliomas and almost 85% of oligoastrocytomas were reclassified as astrocytomas.

Table 1 summarizes patient demographics, histopathology, and molecular genetic status.

Table 1 Patient demographics, histopathology, and molecular genetic status

	Total ($n = 71$)	Oligodendroglioma ($n = 33$)	Astrocytoma ($n = 38$)
Age, mean (SD) (years)	48 (11.2)	49 (11.3)	38 (12.1)
Female sex (no.)	36 (52.2%)	19 (57.6%)	17 (47.2%)
Tumor grade			
WHO II	42 (59.1%)	23 (54.7%)	19 (45.3%)
WHO III	29 (40.9%)	10 (34.4%)	19 (65.6%)
Known IDH mutation status	43 (57.7%)	18 (41.9%)	25 (58.1%)
IDH—mutant	41 (95.3%)	18 (100%)	23 (92%)
IDH—wild type	2 (4.6%)		2 (8%)

DSC-MRI and DWI histogram parameters for differentiation between oligodendrogliomas and astrocytomas

Detailed results for DSC-MRI and DWI parameters based on histogram analysis to distinguish oligodendrogliomas from astrocytomas are summarized in Table S1. ROC analysis with suggested optimal cutoff value and estimated positive and negative predictive values for each of parameters with significant probability values is given in Table 2.

Oligodendrogliomas showed a significantly higher $rCBV_{Mean}$ and lower $rCBV_{Peak}$ compared to diffuse astrocytomas ($p = 0.013$; $p = 0.015$, respectively). ROC analysis yielded AUC values of 77% using the parameter $rCBV_{Mean}$ and 80% for the parameter $rCBV_{Peak}$, respectively, for discrimination of oligodendrogliomas from diffuse astrocytomas. Figure 3 illustrates average $rCBV_{Peak}$ histograms for all oligodendrogliomas and astrocytomas regardless of grade.

Diffuse gliomas with lower ADC_{Mean} were more likely to be oligodendroglioma rather than astrocytoma ($p = 0.009$). Higher ADC_{Peak} and lower ADC_{Mean} indicated oligodendroglioma when the glioma grade II subgroup was analyzed separately ($p = 0.042$; $p = 0.001$, respectively).

Figure 4 demonstrates boxplots with distribution range of $rCBV_{Peak}$, $rCBV_{Mean}$, and ADC_{Mean} values in different subgroups of diffuse gliomas.

In our study, the linear combination of most significant variables ($rCBV_{Peak}$, $rCBV_{Mean}$, and ADC_{Mean}) based on logistic regression had the superior diagnostic performance in differentiating oligodendrogliomas from diffuse astrocytomas. ROC analysis yielded AUC value of 84% (Table 2, Fig. 5). In LOOCV, this combined predictive model have 28% error rate when all gliomas were included and 21% in grade II gliomas subtype; however, misclassification rate was increased to 42% when just grade III gliomas were analyzed.

Table 2 Results of ROC curve analysis and error rate estimated using leave-one-out cross-validation of DWI and DSC-MRI histogram-derived parameters in patients with diffuse glioma grade II and III

	Cutoff points	Sensitivity % (95% CI)	Specificity % (95% CI)	Positive predictive value % (95% CI)	Negative predictive value % (95% CI)	AUC	Error rate (%)**
Oligodendroglioma vs astrocytoma (WHO grade II and III)							
ADC_{Mean}	$\leq 1094 \times 10^{-6}$ mm^2/s	63 (54; 82)	61 (51; 83)	65 (52; 81)	73 (61; 87)	76	32
$rCBV_{Peak}$	≤ 0.044	78 (56; 82)	78 (54; 93)	76 (63; 88)	76 (63; 88)	80	30
$rCBV_{Mean}$	≥ 0.80 mL/100 g	68 (52; 90)	93 (69; 99)	65 (48; 83)	92 (70; 98)	77	32
Linear combination based on logistic regression*		92 (62; 96)	81 (69; 99)	88 (62; 96)	80 (70; 98)	84	28
Oligodendroglioma vs astrocytoma (WHO grade II)							
ADC_{Peak}	≥ 0.043	57 (37; 75)	95 (68; 99)	54 (36; 75)	94 (70; 98)	69	36
ADC_{Mean}	$\leq 1101 \times 10^{-6}$ mm^2/s	84 (70; 93)	65 (47; 82)	85 (70; 93)	67 (49; 82)	75	33
Oligodendroglioma vs astrocytoma (WHO grade III)							
$rCBV_{Peak}$	≤ 0.046	68 (49; 85)	73 (61; 87)	65 (46; 81)	72 (61; 87)	73	34

CI confidence interval, *AUC* area under the curve

*Linear combination included most significant variables: ADC_{Mean}, $rCBV_{Mean}$, and $rCBV_{Peak}$

**Error rate was estimated using leave-one-out cross-validation

Fig. 3 Whole-volume average $rCBV_{Peak}$ histograms (± 1.96 standard error of mean (SEM)) of all oligodendroglioma and astrocytomas WHO grades II and III
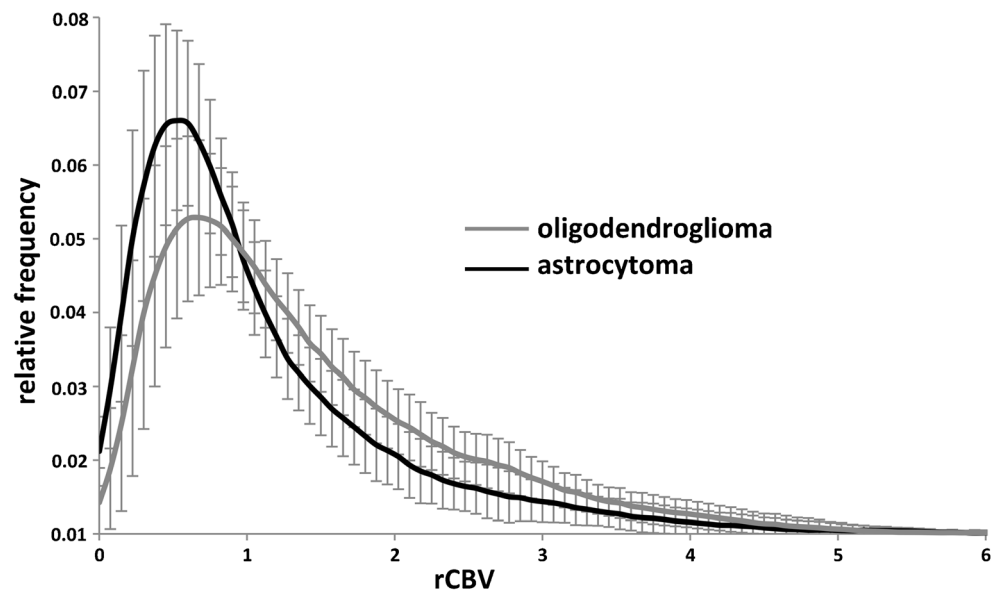
DSC-MRI and DWI histogram parameters for differentiation between WHO grade II and grade III

The correlations between $rCBV_{Peak}$, $rCBV_{Mean}$, ADC_{Peak}, and ADC_{Mean} and WHO grade are demonstrated in Table S2. There was a substantial overlap in rCBV and ADC histogram-derived biomarkers between WHO glioma grade II and III, and no significant differences were observed in the univariate model. LOOCV performed with inclusion of these four parameters showed also high error rate (49%). In the multivariate regression model, the value of ADC_{Mean} was an independent variable for discriminating between astrocytoma WHO grades II and III ($p = 0.03$). The odds of astrocytoma WHO grade III increased in low ADC_{Mean} lesions (OR, 0.92 for each unit decrease in ADC_{Mean} with 95% CI, 0.82–0.98).

Discussion

In our study, we identified microvascularity parameters suggesting a denser and more heterogeneous vascular distribution in oligodendrogliomas compared to those of astrocytomas. Measures of rCBV parameters showed fair diagnostic performance and further improved diagnostic value in combination with ADC parameters for discriminating oligodendroglioma from astrocytoma.

Our results imply that histogram-derived rCBV and ADC values could be useful imaging biomarkers for differentiating these two types of diffuse glioma. Non-invasive biomarkers are of special relevance in cases with ambiguous biopsy results, deep-seated inoperable tumors, and in patients with primary or recurrent tumors where a "wait-and-see" management is pursued. Moreover, identification of oligodendroglioma is also
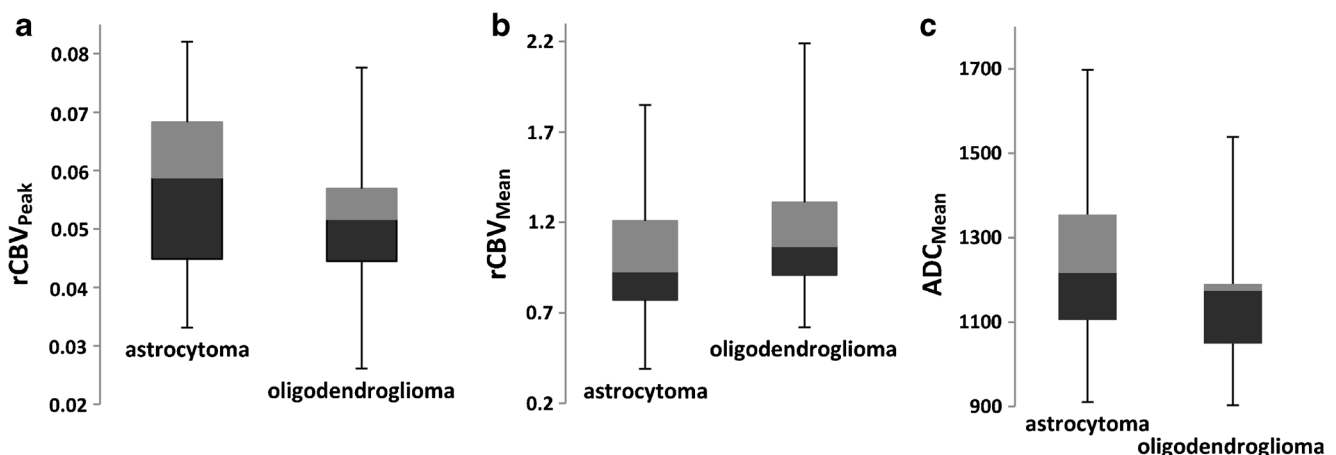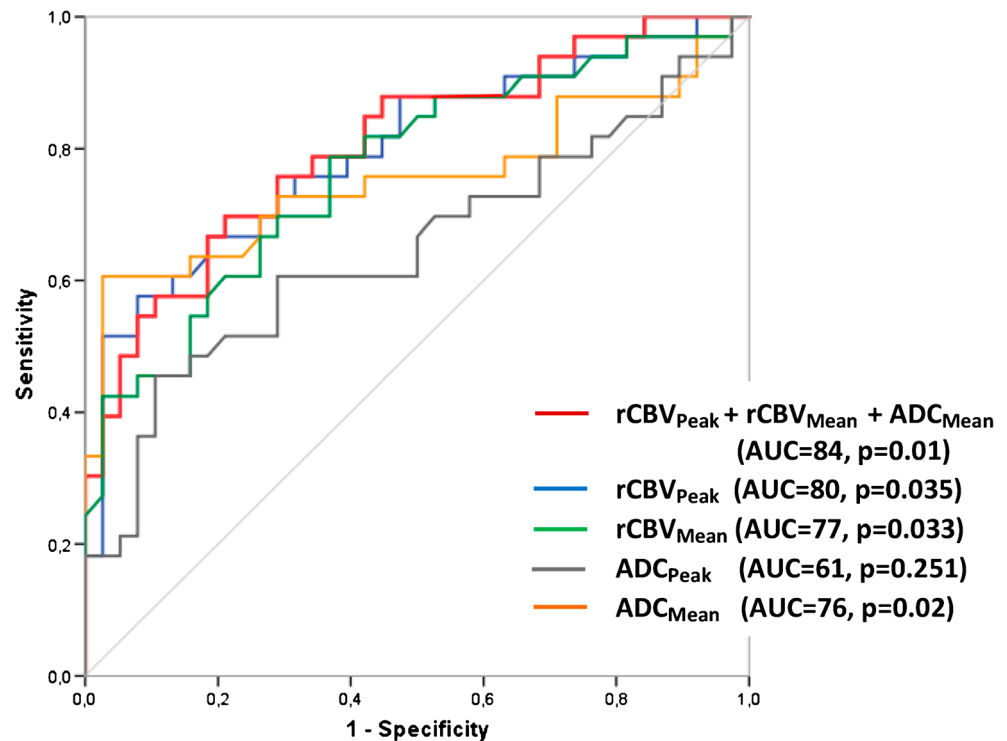

Fig. 4 Boxplots with distribution range of **a** $rCBV_{Peak}$, **b** $rCBV_{Mean}$, and **c** ADC_{Mean} values in different subgroups of diffuse gliomas

Fig. 5 Receiver operating characteristic (ROC) curves for imaging derived histogram biomarkers (rCBV$_{Peak}$, rCBV$_{Mean}$, ADC$_{Mean}$, ADC$_{Peak}$) used to identify oligodendroglioma

of importance for the choice of therapeutic strategy. Patients with oligodendroglial tumor grade III have been shown to benefit from procarbazine, lomustine, and vincristine (PCV), whereas in patients with astrocytoma grade III, temozolomide has been shown to be beneficial [1, 2].

The key finding in our study is higher vascularity (high rCBV$_{Mean}$) in oligodendrogliomas as compared to astrocytomas, regardless of histopathological grade. A few retrospective studies have attempted to correlate 1p19q codeletion with rCBV and have demonstrated findings similar to ours [19, 26]. Jenkinson et al. showed that rCBV > 1.59 predicted 1p/19q status with 92% sensitivity and 76% specificity [18]. In contrast to our results, Yoon et al. found that the volume transfer coefficient (K^{trans}), extravascular extracellular distribution volume (V_e), and rCBV values were not significantly different between the oligodendroglioma group and grade II/III astrocytoma group [27]. Increased blood volumes in oligodendrogliomas could be explained by higher metabolic demands associated with 1p/19q codeletion [28]. Increased F-FDG uptake was demonstrated in positron emission tomography and single-photon emission computed tomography studies [28, 29]. Moreover, high intratumoral metabolism may also explain increased sensitivity to chemotherapy. It was suggested that alkylating agents exert a more beneficial effect in tumors with higher cell turnover and DNA synthesis rates, which are known to correlate with higher glucose utilization and metabolism [30, 31]. We did not observe differences

in vascular densities between oligodendroglioma and astrocytoma in grade II tumors. While this result is based on the new WHO classification, our finding corroborates previous work and suggests that 1p/19q codeletion alone is not categorically linked to vascular status and apparent neoangiogenesis in low-grade tumors. Instead, our data also suggest higher vascular heterogeneity (low rCBV$_{Peak}$) in oligodendrogliomas compared to astrocytomas regardless of tumor grade. This idea is also consistent with previous findings from our group [15], as well as that of Cha et al. who also showed that rCBVmax measurements varied greatly within each individual oligodendroglioma (1.29 to 9.24), whereas astrocytomas tended to have little relative variation (0.48 to 1.34) [32].

Another important finding in our study was the higher cellular density (low ADC$_{Mean}$) in patients with oligodendroglioma compared to astrocytoma. These results parallel those of previous studies reporting lower maximum ADC, and a lower mean histogram ADC, in tumors with 1p/19q loss compared to those without [16, 17, 33]. There are several possible explanations for the increase of restrictive diffusion in oligodendroglioma. One of them is the presence of calcification which is common in oligodendroglioma and may limit water content as well as and hinder water movement [34]. Classical oligodendroglial tumors are often highly cellular lesions with closely packed, relatively small cells in central regions and prominent secondary structure formation, such as clustering of tumor cells around the

perikarya of preexisting neurons (satellitosis) and surrounding cortical small vessels (perivascular aggregates) [35]. These formations may also delay passage of small molecules as they need to navigate around cellular obstacles.

In our study, ADC_{Peak} and ADC_{Mean} values were not significantly different between oligodendroglioma grade II and oligodendroglioma grade III. Our findings therefore do not seem to corroborate those of Lin et al. who reported a significantly lower normalized ADC in high-grade oligodendrogliomas compared to low-grade oligodendrogliomas [36]. These differences, however, may be explained through differences in methodology (hotspot method vs histogram approach).

Other authors have demonstrated that tumors with 1p/19q codeletion tend to have a narrow histogram peak (higher ADC_{Peak}) indicating greater homogeneity, compared to tumors with intact 1p/19q [17]. In our study, this association was observed just for grade II tumors, a finding that most likely may be explained by higher numbers of edematous areas, hemorrhage, and cystic or mucinous degeneration in anaplastic tumors compared to low-grade tumors.

Moreover, we found that combined use of ADC and rCBV histogram parameters also improved the ability to identify oligodendroglial from astrocytic tumors. This result is in line with those of a recently published study that found that ADC in combination with rCBV, T2 volume enhancement, and contrast enhancement distinguished IDH mutant/1p19q codeleted from IDH mutant/1p19q non-codeleted gliomas [37]. In contradiction, neither rCBV nor ADC parameters could distinguish between histopathologic grades in diffuse gliomas as previously suggested [38].

Our study has limitations. First, two different assays (FISH and MLPA) were used for detection of 1p and 19q deletions in tumoral tissue. 1p/19q codeletion as detected by FISH could in principle be loss of alleles and not the whole arms, thereby yielding false positive results. Although MLPA in principle is more sensitive and less dependent on individual interpretation than FISH, both technologies have showed concordant results in validation studies [6, 39]. Second, there is a risk of classification errors in histopathological diagnoses of tumor samples derived from biopsies, particularly with regard to the differentiation between grade II and grade III gliomas [8, 40]. Third, our study may also be limited by the preselection of patients with histological oligodendroglial features only. Fourth, IDH1/2 status was not available in all the patients (57.7% of patients cohort). However, a large number of studies show that IDH1/2 mutation occurs in all 1p19q-codeleted tumors and the great majority of diffuse glioma grade II/III also falls into the IDH mutant category [6, 7, 41–45]. Finally, as is true across all imaging modalities, the manual tumor outlining performed in our study is subjective and reproducibility may be challenged when used in combination with

advanced imaging techniques. However, the high intraobserver agreement of the histogram method suggests that subtle changes in ROI editing are relatively unimportant, given the large number of data points included in the histogram [23].

In conclusion, non-invasive glioma assessment is an important supplement to neuropathological evaluation in newly diagnosed disease and longitudinal follow-up. Histograms derived DSC-MRI, and DWI parameters may be used as non-invasive imaging biomarkers for identification of oligodendroglioma as defined by the new WHO 2016 classification criteria.

Compliance with ethical standards

Conflict of interest KEE has intellectual property rights with NordicNeuroLaB, Bergen Oslo.

Ethical approval All procedures performed in the studies involving human participants were in accordance with the ethical standards of the institutional and/or national research committee and with the 1964 Helsinki Declaration and its later amendments or comparable ethical standards.

Informed consent Informed consent was obtained from all individual participants included in the study.

Publisher's note Springer Nature remains neutral with regard to jurisdictional claims in published maps and institutional affiliations.

References

1. van den Bent MJ, Brandes AA, Taphoorn MJ, Kros JM, Kouwenhoven MC, Delattre JY, Bernsen HJ, Frenay M, Tijssen CC, Grisold W, Sipos L, Enting RH, French PJ, Dinjens WN, Vecht CJ, Allgeier A, Lacombe D, Gorlia T, Hoang-Xuan K (2013) Adjuvant procarbazine, lomustine, and vincristine chemotherapy in newly diagnosed anaplastic oligodendroglioma: long-term follow-up of EORTC brain tumor group study 26951. J Clin Oncol 31(3):344–350. https://doi.org/10.1200/jco.2012.43.2229

2. Cairncross G, Wang M, Shaw E, Jenkins R, Brachman D, Buckner J, Fink K, Souhami L, Laperriere N, Curran W, Mehta M (2013) Phase III trial of chemoradiotherapy for anaplastic oligodendroglioma: long-term results of RTOG 9402. J Clin Oncol 31(3):337–343. https://doi.org/10.1200/jco.2012.43.2674

3. Buckner JC, Shaw EG, Pugh SL, Chakravarti A, Gilbert MR, Barger GR, Coons S, Ricci P, Bullard D, Brown PD, Stelzer K, Brachman D, Suh JH, Schultz CJ, Bahary JP, Fisher BJ, Kim H, Murtha AD, Bell EH, Won M, Mehta MP, Curran WJ Jr (2016) Radiation plus procarbazine, CCNU, and vincristine in low-grade

glioma. N Engl J Med 374(14):1344–1355. https://doi.org/10.1056/NEJMoa1500925

4. Sanson M, Marie Y, Paris S, Idbaih A, Laffaire J, Ducray F, El Hallani S, Boisselier B, Mokhtari K, Hoang-Xuan K, Delattre JY (2009) Isocitrate dehydrogenase 1 codon 132 mutation is an important prognostic biomarker in gliomas. J Clin Oncol 27(25):4150–4154. https://doi.org/10.1200/jco.2009.21.9832

5. Louis DN, Perry A, Reifenberger G, von Deimling A, Figarella-Branger D, Cavenee WK, Ohgaki H, Wiestler OD, Kleihues P, Ellison DW (2016) The 2016 World Health Organization Classification of Tumors of the Central Nervous System: a summary. Acta Neuropathol 131(6):803–820. https://doi.org/10.1007/s00401-016-1545-1

6. Ballester LY, Huse JT, Tang G, Fuller GN (2017) Molecular classification of adult diffuse gliomas: conflicting IDH1/IDH2, ATRX and 1p/19q results. Hum Pathol 69:15–22. https://doi.org/10.1016/j.humpath.2017.05.005

7. Sahm F, Reuss D, Koelsche C, Capper D, Schittenhelm J, Heim S, Jones DT, Pfister SM, Herold-Mende C, Wick W, Mueller W, Hartmann C, Paulus W, von Deimling A (2014) Farewell to oligoastrocytoma: in situ molecular genetics favor classification as either oligodendroglioma or astrocytoma. Acta Neuropathol 128(4):551–559. https://doi.org/10.1007/s00401-014-1326-7

8. Giannini C, Scheithauer BW, Weaver AL, Burger PC, Kros JM, Mork S, Graeber MB, Bauserman S, Buckner JC, Burton J, Riepe R, Tazelaar HD, Nascimento AG, Crotty T, Keeney GL, Pernicone P, Altermatt H (2001) Oligodendrogliomas: reproducibility and prognostic value of histologic diagnosis and grading. J Neuropathol Exp Neurol 60(3):248–262

9. Lev MH, Ozsunar Y, Henson JW, Rasheed AA, Barest GD, Harsh GR, Fitzek MM, Chiocca EA, Rabinov JD, Csavoy AN, Rosen BR, Hochberg FH, Schaefer PW, Gonzalez RG (2004) Glial tumor grading and outcome prediction using dynamic spin-echo MR susceptibility mapping compared with conventional contrast-enhanced MR: confounding effect of elevated rCBV of oligodendrogliomas [corrected]. AJNR Am J Neuroradiol 25(2):214–221

10. Law M, Oh S, Babb JS, Wang E, Inglese M, Zagzag D, Knopp EA, Johnson G (2006) Low-grade gliomas: dynamic susceptibility-weighted contrast-enhanced perfusion MR imaging–prediction of patient clinical response. Radiology 238(2):658–667. https://doi.org/10.1148/radiol.2382042180

11. Knopp EA, Cha S, Johnson G, Mazumdar A, Golfinos JG, Zagzag D, Miller DC, Kelly PJ, Kricheff II (1999) Glial neoplasms: dynamic contrast-enhanced T2*-weighted MR imaging. Radiology 211(3):791–798. https://doi.org/10.1148/radiology.211.3.r99jn46791

12. Le Bihan D (1991) Molecular diffusion nuclear magnetic resonance imaging. Magn Reson Q 7(1):1–30

13. Kono K, Inoue Y, Nakayama K, Shakudo M, Morino M, Ohata K, Wakasa K, Yamada R (2001) The role of diffusion-weighted imaging in patients with brain tumors. AJNR Am J Neuroradiol 22(6):1081–1088

14. Chawla S, Krejza J, Vossough A, Zhang Y, Kapoor GS, Wang S, O'Rourke DM, Melhem ER, Poptani H (2013) Differentiation between oligodendroglioma genotypes using dynamic susceptibility contrast perfusion-weighted imaging and proton MR spectroscopy. AJNR Am J Neuroradiol 34(8):1542–1549. https://doi.org/10.3174/ajnr.A3384

15. Emblem KE, Scheie D, Due-Tonnessen P, Nedregaard B, Nome T, Hald JK, Beiske K, Meling TR, Bjornerud A (2008) Histogram analysis of MR imaging-derived cerebral blood volume maps: combined glioma grading and identification of low-grade oligodendroglial subtypes. AJNR Am J Neuroradiol 29(9):1664–1670. https://doi.org/10.3174/ajnr.A1182

16. Fellah S, Caudal D, De Paula AM, Dory-Lautrec P, Figarella-Branger D, Chinot O, Metellus P, Cozzone PJ, Confort-Gouny S,

Ghattas B, Callot V, Girard N (2013) Multimodal MR imaging (diffusion, perfusion, and spectroscopy): is it possible to distinguish oligodendroglial tumor grade and 1p/19q codeletion in the pretherapeutic diagnosis? AJNR Am J Neuroradiol 34(7):1326–1333. https://doi.org/10.3174/ajnr.A3352

17. Jenkinson MD, du Plessis DG, Smith TS, Brodbelt AR, Joyce KA, Walker C (2010) Cellularity and apparent diffusion coefficient in oligodendroglial tumours characterized by genotype. J Neuro-Oncol 96(3):385–392. https://doi.org/10.1007/s11060-009-9970-9

18. Jenkinson MD, Smith TS, Joyce KA, Fildes D, Broome J, du Plessis DG, Haylock B, Husband DJ, Warnke PC, Walker C (2006) Cerebral blood volume, genotype and chemosensitivity in oligodendroglial tumours. Neuroradiology 48(10):703–713. https://doi.org/10.1007/s00234-006-0122-z

19. Whitmore RG, Krejza J, Kapoor GS, Huse J, Woo JH, Bloom S, Lopinto J, Wolf RL, Judy K, Rosenfeld MR, Biegel JA, Melhem ER, O'Rourke DM (2007) Prediction of oligodendroglial tumor subtype and grade using perfusion weighted magnetic resonance imaging. J Neurosurg 107(3):600–609. https://doi.org/10.3171/jns-07/09/0600

20. Louis DN, Ohgaki H, Wiestler OD, Cavenee WK, Burger PC, Jouvet A, Scheithauer BW, Kleihues P (2007) The 2007 WHO classification of tumours of the central nervous system. Acta Neuropathol 114(2):97–109. https://doi.org/10.1007/s00401-007-0243-4

21. Scheie D, Andresen PA, Cvancarova M, Bo AS, Helseth E, Skullerud K, Beiske K (2006) Fluorescence in situ hybridization (FISH) on touch preparations: a reliable method for detecting loss of heterozygosity at 1p and 19q in oligodendroglial tumors. Am J Surg Pathol 30(7):828–837. https://doi.org/10.1097/01.pas.0000213250.44822.2e

22. Natte R, van Eijk R, Eilers P, Cleton-Jansen AM, Oosting J, Kouwenhove M, Kros JM, van Duinen S (2005) Multiplex ligation-dependent probe amplification for the detection of 1p and 19q chromosomal loss in oligodendroglial tumors. Brain Pathol (Zurich, Switzerland) 15(3):192–197

23. Emblem KE, Nedregaard B, Nome T, Due-Tonnessen P, Hald JK, Scheie D, Borota OC, Cvancarova M, Bjornerud A (2008) Glioma grading by using histogram analysis of blood volume heterogeneity from MR-derived cerebral blood volume maps. Radiology 247(3):808–817. https://doi.org/10.1148/radiol.2473070571

24. Emblem KE, Pinho MC, Zollner FG, Due-Tonnessen P, Hald JK, Schad LR, Meling TR, Rapalino O, Bjornerud A (2015) A generic support vector machine model for preoperative glioma survival associations. Radiology 275(1):228–234. https://doi.org/10.1148/radiol.14140770

25. Pope WB, Kim HJ, Huo J, Alger J, Brown MS, Gjertson D, Sai V, Young JR, Tekchandani L, Cloughesy T, Mischel PS, Lai A, Nghiemphu P, Rahmanuddin S, Goldin J (2009) Recurrent glioblastoma multiforme: ADC histogram analysis predicts response to bevacizumab treatment. Radiology 252(1):182–189. https://doi.org/10.1148/radiol.2521081534

26. Kapoor GS, Gocke TA, Chawla S, Whitmore RG, Nabavizadeh A, Krejza J, Lopinto J, Plaum J, Maloney-Wilensky E, Poptani H, Melhem ER, Judy KD, O'Rourke DM (2009) Magnetic resonance perfusion-weighted imaging defines angiogenic subtypes of oligodendroglioma according to 1p19q and EGFR status. J Neuro-Oncol 92(3):373–386. https://doi.org/10.1007/s11060-009-9880-x

27. Yoon HJ, Ahn KJ, Lee S, Jang JH, Choi HS, Jung SL, Kim BS, Jeun SS, Hong YK (2017) Differential diagnosis of oligodendroglial and astrocytic tumors using imaging results: the added value of perfusion MR imaging. Neuroradiology 59:665–675. https://doi.org/10.1007/s00234-017-1851-x

28. Walker C, Haylock B, Husband D, Joyce KA, Fildes D, Jenkinson MD, Smith T, Broome J, Kopitzki K, du Plessis DG, Prosser J,

Vinjamuri S, Warnke PC (2006) Genetic and metabolic predictors of chemosensitivity in oligodendroglial neoplasms. Br J Cancer 95(10):1424–1431. https://doi.org/10.1038/sj.bjc.6603390

29. Shinozaki N, Uchino Y, Yoshikawa K, Matsutani T, Hasegawa A, Saeki N, Iwadate Y (2011) Discrimination between low-grade oligodendrogliomas and diffuse astrocytoma with the aid of 11C-methionine positron emission tomography. J Neurosurg 114(6): 1640–1647. https://doi.org/10.3171/2010.11.jns10553

30. Herholz K, Pietrzyk U, Voges J, Schroder R, Halber M, Treuer H, Sturm V, Heiss WD (1993) Correlation of glucose consumption and tumor cell density in astrocytomas. A stereotactic PET study. J Neurosurg 79(6):853–858. https://doi.org/10.3171/jns.1993.79.6.0853

31. Brock CS, Young H, O'Reilly SM, Matthews J, Osman S, Evans H, Newlands ES, Price PM (2000) Early evaluation of tumour metabolic response using [18F]fluorodeoxyglucose and positron emission tomography: a pilot study following the phase II chemotherapy schedule for temozolomide in recurrent high-grade gliomas. Br J Cancer 82(3):608–615. https://doi.org/10.1054/bjoc.1999.0971

32. Cha S, Tihan T, Crawford F, Fischbein NJ, Chang S, Bollen A, Nelson SJ, Prados M, Berger MS, Dillon WP (2005) Differentiation of low-grade oligodendrogliomas from low-grade astrocytomas by using quantitative blood-volume measurements derived from dynamic susceptibility contrast-enhanced MR imaging. AJNR Am J Neuroradiol 26(2):266–273

33. Johnson DR, Diehn FE, Giannini C, Jenkins RB, Jenkins SM, Parney IF, Kaufmann TJ (2017) Genetically defined oligodendroglioma is characterized by indistinct tumor borders at MRI. AJNR Am J Neuroradiol 38:678–684. https://doi.org/10.3174/ajnr.A5070

34. Smits M (2016) Imaging of oligodendroglioma. Br J Radiol 89(1060):20150857. https://doi.org/10.1259/bjr.20150857

35. Wesseling P, van den Bent M, Perry A (2015) Oligodendroglioma: pathology, molecular mechanisms and markers. Acta Neuropathol 129(6):809–827. https://doi.org/10.1007/s00401-015-1424-1

36. Lin Y, Xing Z, She D, Yang X, Zheng Y, Xiao Z, Wang X, Cao D (2017) IDH mutant and 1p/19q co-deleted oligodendrogliomas: tumor grade stratification using diffusion-, susceptibility-, and perfusion-weighted MRI. Neuroradiology 59(6):555–562. https://doi.org/10.1007/s00234-017-1839-6

37. Leu K, Ott GA, Lai A, Nghiemphu PL, Pope WB, Yong WH, Liau LM, Cloughesy TF, Ellingson BM (2017) Perfusion and diffusion MRI signatures in histologic and genetic subtypes of WHO grade II-III diffuse gliomas. J Neuro-Oncol 134:177–188. https://doi.org/10.1007/s11060-017-2506-9

38. Delgado AF, Delgado AF (2017) Discrimination between glioma grades II and III using dynamic susceptibility perfusion MRI: a meta-analysis. AJNR Am J Neuroradiol 38(7):1348–1355. https://doi.org/10.3174/ajnr.A5218

39. Franco-Hernandez C, Martinez-Glez V, de Campos JM, Isla A, Vaquero J, Gutierrez M, Casartelli C, Rey JA (2009) Allelic status of 1p and 19q in oligodendrogliomas and glioblastomas: multiplex ligation-dependent probe amplification versus loss of heterozygosity. Cancer Genet Cytogenet 190(2):93–96. https://doi.org/10.1016/j.cancergencyto.2008.09.017

40. van den Bent MJ (2010) Interobserver variation of the histopathological diagnosis in clinical trials on glioma: a clinician's perspective. Acta Neuropathol 120(3):297–304. https://doi.org/10.1007/s00401-010-0725-7

41. Kim SI, Lee Y, Won JK, Park CK, Choi SH, Park SH (2017) Reclassification of mixed oligoastrocytic tumors using a genetically integrated diagnostic approach. J Pathol Transl Med 52:28–36. https://doi.org/10.4132/jptm.2017.09.25

42. Brat DJ, Verhaak RG, Aldape KD, Yung WK, Salama SR, Cooper LA, Rheinbay E, Miller CR, Vitucci M, Morozova O, Robertson AG, Noushmehr H, Laird PW, Cherniack AD, Akbani R, Huse JT, Ciriello G, Poisson LM, Barnholtz-Sloan JS, Berger MS, Brennan C, Colen RR, Colman H, Flanders AE, Giannini C, Grifford M, Iavarone A, Jain R, Joseph I, Kim J, Kasaian K, Mikkelsen T, Murray BA, O'Neill BP, Pachter L, Parsons DW, Sougnez C, Sulman EP, Vandenberg SR, Van Meir EG, von Deimling A, Zhang H, Crain D, Lau K, Mallery D, Morris S, Paulauskis J, Penny R, Shelton T, Sherman M, Yena P, Black A, Bowen J, Dicostanzo K, Gastier-Foster J, Leraas KM, Lichtenberg TM, Pierson CR, Ramirez NC, Taylor C, Weaver S, Wise L, Zmuda E, Davidsen T, Demchok JA, Eley G, Ferguson ML, Hutter CM, Mills Shaw KR, Ozenberger BA, Sheth M, Sofia HJ, Tarnuzzer R, Wang Z, Yang L, Zenklusen JC, Ayala B, Baboud J, Chudamani S, Jensen MA, Liu J, Pihl T, Raman R, Wan Y, Wu Y, Ally A, Auman JT, Balasundaram M, Balu S, Baylin SB, Beroukhim R, Bootwalla MS, Bowlby R, Bristow CA, Brooks D, Butterfield Y, Carlsen R, Carter S, Chin L, Chu A, Chuah E, Cibulskis K, Clarke A, Coetzee SG, Dhalla N, Fennell T, Fisher S, Gabriel S, Getz G, Gibbs R, Guin R, Hadjipanayis A, Hayes DN, Hinoue T, Hoadley K, Holt RA, Hoyle AP, Jefferys SR, Jones S, Jones CD, Kucherlapati R, Lai PH, Lander E, Lee S, Lichtenstein L, Ma Y, Maglinte DT, Mahadeshwar HS, Marra MA, Mayo M, Meng S, Meyerson ML, Mieczkowski PA, Moore RA, Mose LE, Mungall AJ, Pantazi A, Parfenov M, Park PJ, Parker JS, Perou CM, Protopopov A, Ren X, Roach J, Sabedot TS, Schein J, Schumacher SE, Seidman JG, Seth S, Shen H, Simons JV, Sipahimalani P, Soloway MG, Song X, Sun H, Tabak B, Tam A, Tan D, Tang J, Thiessen N, Triche T Jr, Van Den Berg DJ, Veluvolu U, Waring S, Weisenberger DJ, Wilkerson MD, Wong T, Wu J, Xi L, Xu AW, Yang L, Zack TI, Zhang J, Aksoy BA, Arachchi H, Benz C, Bernard B, Carlin D, Cho J, DiCara D, Frazer S, Fuller GN, Gao J, Gehlenborg N, Haussler D, Heiman DI, Iype L, Jacobsen A, Ju Z, Katzman S, Kim H, Knijnenburg T, Kreisberg RB, Lawrence MS, Lee W, Leinonen K, Lin P, Ling S, Liu Y, Liu Y, Liu Y, Lu Y, Mills G, Ng S, Noble MS, Paull E, Rao A, Reynolds S, Saksena G, Sanborn Z, Sander C, Schultz N, Senbabaoglu Y, Shen R, Shmulevich I, Sinha R, Stuart J, Sumer SO, Sun Y, Tasman N, Taylor BS, Voet D, Weinhold N, Weinstein JN, Yang D, Yoshihara K, Zheng S, Zhang W, Zou L, Abel T, Sadeghi S, Cohen ML, Eschbacher J, Hattab EM, Raghunathan A, Schniederjan MJ, Aziz D, Barnett G, Barrett W, Bigner DD, Boice L, Brewer C, Calatozzolo C, Campos B, Carlotti CG Jr, Chan TA, Cuppini L, Curley E, Cuzzubbo S, Devine K, DiMeco F, Duell R, Elder JB, Fehrenbach A, Finocchiaro G, Friedman W, Fulop J, Gardner J, Hermes B, Herold-Mende C, Jungk C, Kendler A, Lehman NL, Lipp E, Liu O, Mandt R, McGraw M, McLendon R, McPherson C, Neder L, Nguyen P, Noss A, Nunziata R, Ostrom QT, Palmer C, Perin A, Pollo B, Potapov A, Potapova O, Rathmell WK, Rotin D, Scarpace L, Schilero C, Senecal K, Shimmel K, Shurkhay V, Sifri S, Singh R, Sloan AE, Smolenski K, Staugaitis SM, Steele R, Thorne L, Tirapelli DP, Unterberg A, Vallurupalli M, Wang Y, Warnick R, Williams F, Wolinsky Y, Bell S, Rosenberg M, Stewart C, Huang F, Grimsby JL, Radenbaugh AJ, Zhang J (2015) Comprehensive, integrative genomic analysis of diffuse lower-grade gliomas. N Engl J Med 372(26):2481–2498. https://doi.org/10.1056/NEJMoa1402121

43. Valera-Mele M, Mateo Sierra O, Sola Vendrell E, Guzman de Villoria LJ, Carvajal Diaz L, Gil de Sagredo Del Corral OL, Garcia Leal R (2018) Evaluación del impacto del cambio diagnóstico de los gliomas aplicando la nueva clasificación de la OMS de 2016 sobre una serie de casos. In: Assessment of the impact of glioma diagnostic reclassification following the new 2016 WHO classification on a series of cases. Neurocirugia. https://doi.org/10.1016/j.neucir.2018.09.002

44. van den Bent MJ, Smits M, Kros JM, Chang SM (2017) Diffuse infiltrating oligodendroglioma and astrocytoma. J Clin Oncol 35(21):2394–2401. https://doi.org/10.1200/jco.2017.72.6737

45. Eckel-Passow JE, Lachance DH, Molinaro AM, Walsh KM, Decker PA, Sicotte H, Pekmezci M, Rice T, Kosel ML, Smirnov IV, Sarkar G, Caron AA, Kollmeyer TM, Praska CE, Chada AR, Halder C, Hansen HM, McCoy LS, Bracci PM, Marshall R, Zheng S, Reis GF, Pico AR, O'Neill BP, Buckner JC, Giannini C, Huse JT, Perry A, Tihan T, Berger MS, Chang SM, Prados MD, Wiemels J, Wiencke JK, Wrensch MR, Jenkins RB (2015) Glioma groups based on 1p/19q, IDH, and TERT promoter mutations in tumors. N Engl J Med 372(26):2499–2508. https://doi.org/10.1056/NEJMoa1407279

46. Gadji M, Fortin D, Tsanaclis AM, Drouin R (2009) Is the 1p/19q deletion a diagnostic marker of oligodendrogliomas? Cancer Genet Cytogenet 194(1):12–22. https://doi.org/10.1016/j.cancergencyto.2009.05.004

47. Waitkus MS, Diplas BH, Yan H (2016) Isocitrate dehydrogenase mutations in gliomas. Neuro-Oncology 18(1):16–26. https://doi.org/10.1093/neuonc/nov136